POLYPUBLIE
Polytechnique Montréal

POLYTECHNIQUE MONTRÉAL
UNIVERSITÉ D'INGÉNIERIE

Titre: Title:	Effect of blending sequence and epoxy functionalized compatibilizer on barrier and mechanical properties of PBS and PBS/PLA nanocomposite blown films
Auteurs: Authors:	Salima Adrar, & Abdellah Ajji
Date:	2024
Type:	Article de revue / Article
Référence: Citation:	Adrar, S., & Ajji, A. (2024). Effect of blending sequence and epoxy functionalized compatibilizer on barrier and mechanical properties of PBS and PBS/PLA nanocomposite blown films. Journal of Vinyl and Additive Technology, 12 pages. https://doi.org/10.1002/vnl.22092

Document en libre accès dans PolyPublie
Open Access document in PolyPublie

URL de PolyPublie: PolyPublie URL:	https://publications.polymtl.ca/57553/
Version:	Version officielle de l'éditeur / Published version Révisé par les pairs / Refereed
Conditions d'utilisation: Terms of Use:	CC BY-NC-ND

Document publié chez l'éditeur officiel
Document issued by the official publisher

Titre de la revue: Journal Title:	Journal of Vinyl and Additive Technology
Maison d'édition: Publisher:	Wiley
URL officiel: Official URL:	https://doi.org/10.1002/vnl.22092
Mention légale: Legal notice:	

Ce fichier a été téléchargé à partir de PolyPublie, le dépôt institutionnel de Polytechnique Montréal
This file has been downloaded from PolyPublie, the institutional repository of Polytechnique Montréal

https://publications.polymtl.ca

Check for updates

Received: 20 December 2023 | Revised: 24 January 2024 | Accepted: 24 January 2024

DOI: 10.1002/vnl.22092

RESEARCH ARTICLE

JOURNAL OF Vinyl & Additive TECHNOLOGY WILEY

Effect of blending sequence and epoxy functionalized compatibilizer on barrier and mechanical properties of PBS and PBS/PLA nanocomposite blown films

Salima Adrar | **Abdellah Ajji**

Département de Génie Chimique, Polytechnique Montréal, CREPEC, Montreal, Quebec, Canada

Correspondence
Abdellah Ajji, Département de Génie Chimique, Polytechnique Montréal, CREPEC, C. P. 6079, Succ. Centre-Ville Montréal, QC H3C 3A7, Canada.
Email: abdellah.ajji@polymtl.ca

Funding information
Polyexpert Inc; Natural Sciences and Engineering Research Council of Canada

Abstract

This study focuses on developing compostable nanocomposite blown films, aiming to enhance oxygen barrier properties while maintaining good mechanical performance. Polybutylene succinate (PBS) and its blend with polylactic acid (PLA) were selected as matrices for the films. Organo-montmorillonite Delite®43B (D43B) clay was incorporated to improve oxygen barrier, and random ethylene-methyl acrylate-glycidyl methacrylate terpolymer served as a plasticizer and reactive compatibilizer. Different blending sequences were examined to determine the optimal one that led to significant enhancements in both the barrier and mechanical properties of the final nanocomposite blown film. Various techniques, including SEM, TEM, XRD, DSC, oxygen permeability, and tensile testing were employed to characterize the morphology of the compounds and blown films. The results reveal greater oxygen barrier properties depending on the blending sequence. Indeed, a reduction in oxygen permeability exceeding 50% was observed following the addition of 3 wt% of D43B to the PBS/PLA film, selectively localized in the PLA phase. This enhancement further intensified after the addition of 5 wt% of the epoxy functionalized compatibilizer.

Highlights

- Enhancing PLA-PBS compatibility with the epoxy functionalized compatibilizer led to a reduction in the final film's oxygen permeability.
- Achieving ideal ductility and barrier balance in films requires a synergistic blend of components: D43B, PLA, PBS, and compatibilizer.
- Optimizing balanced synergistic effects among compounds depends on the blending sequence method.

KEYWORDS

blown film, mechanical properties, nanocomposite, oxygen permeability, PBS, PLA, plasticizer

This is an open access article under the terms of the Creative Commons Attribution-NonCommercial-NoDerivs License, which permits use and distribution in any medium, provided the original work is properly cited, the use is non-commercial and no modifications or adaptations are made.
© 2024 The Authors. Journal of Vinyl & Additive Technology published by Wiley Periodicals LLC on behalf of Society of Plastics Engineers.

1 | INTRODUCTION

The relentless issue of plastic pollution continues to cast a shadow over our environment, imperiling ecosystems, and wildlife. The urgency to confront this crisis is particularly pressing in the realm of packaging, with a special focus on food packaging. To combat the escalating environmental concerns linked to non-biodegradable polymers, the integration of biodegradable materials, notably biopolymers such as polylactic acid (PLA), polybutylene succinate (PBS), and poly(butylene succinate-co-adipate), has emerged as a viable strategy.[1,2]

Polylactic acid and polybutylene succinate are two distinct, renewable polymers with unique advantages and limitations. PLA, derived from resources such as corn starch, boasts biodegradability and transparency, making it ideal for transparent packaging. However, it can become brittle at low temperatures and soft at high temperatures, limiting its application, especially in blown film production.[1,2] On the other hand, PBS and PBSA also offer compostability, with high melt strength and thermal stability, making them great for the blown film process.[3] The combination of PBS or PBSA with PLA allows for the fusion of polymer characteristics, such as an increase in the tensile modulus and good elongation at break, all while preserving the biodegradable nature of the resulting material.[1–4] Yet, the challenge of achieving a uniform blend due to the immiscibility of these polymers impacts mechanical properties and overall product performance. Mitigating these issues necessitates a range of techniques, including reactive blending, copolymerization, and modifying polymer chains chemically or physically to enhance compatibility and intermolecular interactions between the polymers.[1,4–6] A commonly employed approach is the addition of reactive compatibilizers, such as lysine triisocyanate,[7] benzoyl peroxide,[8] and ethylene-methyl acrylate-glycidyl methacrylate random terpolymer,[9,10] and so on, which bolster interfacial adhesion between the polymers, facilitating improved blending and overall material quality. Furthermore, the low gas barrier property of these polymers constitutes a critical challenge, especially in their application in food packaging. Multiple strategies are employed to enhance their barrier properties. These include the incorporation of nanocomposites, such as clay nanoparticles, to establish a tortuous path for gas diffusion, as well as the addition of functionalized nanoparticles to enhance compatibility and dispersion within the polymer matrix.[11–17]

The primary challenge lies in delicately balancing different compounds, including clay and plasticizers, within two matrices to achieve the desired properties, emphasizing improved oxygen barrier, mechanical properties and enhanced interfacial adhesion. This delicate balance greatly depends on the sequence blending method, which substantially impacts the final film's properties. The aim of this study is to develop and characterize bio-nanocomposite blown films of PBS and PBS/PLA, with a specific emphasis on enhancing their oxygen barrier and mechanical properties. Delite®43B (D43B) was selected as the nano-clay to enhance the oxygen barrier of both PBS and PBS/PLA films, while random ethylene-methyl acrylate-glycidyl methacrylate terpolymer (ax89) assumed the dual role of a plasticizer to reduce rigidity induced by the presence of D43B or/and PLA, and a reactive compatibilizer to strengthen the interfacial adhesion between PBS and PLA. The plasticizer and D43B were consistently maintained at 5 wt% and 3 wt%, respectively. The research encompassed an evaluation of D43B's morphology and dispersion state in PBS, PBS/PLA nanocomposite films, with and without ax89, employing SEM, XRD, and TEM analysis. Furthermore, the study delved into the examination of crystallinity via DSC analysis, in conjunction with an assessment of the films' oxygen permeability and mechanical properties.

2 | EXPERIMENTAL PART

2.1 | Materials

PBS polybutylene succinate (BioPBS™ FD92PM/FD92PB grade) was supplied by Mitsubishi Chemical Performance Polymers (MCPP). It is bio-based polyester produced from polymerization of bio-based succinic acid and 1,4-butanediol. PBS is semi-crystalline, compostable and flexible grade with excellent properties suitable for both blown and cast film extrusion. Poly(lactic acid) Ingeo 4043D was purchased from NatureWorks (Blair, NE, USA). It is an amorphous grade, specific for film applications, with a molecular weight around 110.000 $g.mol^{-1}$. Lotader®AX8900 (ax89) as a random ethylene-methyl acrylate-glycidyl methacrylate terpolymer was provided from Arkema (SK functional polymer) Investment Co., Ltd (Pennsylvania, USA). The Dellites® 43B (D43B) is an organomontmorillonite which was provided from Laviosa Chimica Mineraria SpA (Italy). According to the supplier, natural bentonite was modified with dimethyl benzyl-hydrogenated tallow ammonium to obtain D43B.

2.2 | Preparation of the samples

Before proceeding with the processing, both the polymers (PLA and PBS) and D43B were subjected to a thorough

15480585, 0, Downloaded from https://4spepublications.onlinelibrary.wiley.com/doi/10.1002/vnl.22092 by Ecole Polytech De Montreal, Wiley Online Library on [09/04/2024]. See the Terms and Conditions (https://onlinelibrary.wiley.com/terms-and-conditions) on Wiley Online Library for rules of use; OA articles are governed by the applicable Creative Commons License

drying process to eliminate any residual moisture. PLA and D43B were dried at 80°C under a vacuum for 8 and 12 h, respectively. PBS and ax89, on the other hand, underwent an overnight drying process under vacuum conditions at 60 and 50°C, respectively. The preparation of the nanocomposite films involved a two-step procedure, detailed in Table 1. Initially, the different nanocomposites were created by simultaneously blending D43B with PLA and/or PBS, with or without the presence of the plasticizer ax89. This blending process took place inside a twin-screw extruder (Leistritz ZSE-18HP-40D, Germany) at a constant speed and a gradually decreasing temperature profile in the presence of PLA, as specified in Table 1. In the second step, the various blends and nanocomposites were used to produce blown films through a single-screw extruder (Labtech Engineering Extrusion Line) featuring a 20 mm diameter, L/D ratio of 30, and a spiral flow die with a 50 mm diameter and a 1 mm opening. The winding speed and the amount of air within the bubble were carefully adjusted to achieve films with a thickness of approximately 55 μm and a lay-flat of 13 cm (Table 2).

2.3 | Characterization

2.3.1 | Scanning electron microscopy (SEM)

The morphology of various sample was observed with a FE-SEM machine (JSM 7600F, JEOL), operated at 2 kV accelerating voltage. The samples were immersed in water beforehand for 2 min and after in nitrogen for around 5 min, then cryo-fractured. Finally, the cryo-fracture surfaces of the different samples were coated with a 15 nm thick gold layer for SEM observations.

2.3.2 | Transmission electron microscopy (TEM)

Transmission electron microscopy model 2100F FEG-TEM (FEG: Field Emission Gun, USA) with an accelerator voltage of 200 kV was used to evaluate the microstructure of different nanocomposites in terms of dispersion and localization of D43B inside the different matrices. The samples were molded in epoxy and cryo-microtomed at room temperature using an ultramicrotome Leica (model EMFC7, USA). The cut slices were 70 nm thick. The reported micrographs represent typical morphologies at least at four different locations.

TABLE 2 Composition and the nomenclature of prepared blown films.

(%)	PBS	ax89	D43B	PLA
PBS	100	-	-	-
PBSax89	95	5	-	
PBSnano	97	-	3	
PBSax89nano	92	5	3	
PBSPLA	70	-	-	30
PBSPLAax89	70	5	-	25
PBS-PLAnano	70	-	30(97PLA:3D43B)	
PBSax89-PLAnano	75(95PBS:5ax89)		25(97PLA:3D43B)	
PBSPLAax89nano	70	5	22	3

TABLE 1 Parameters and steps used for the production of different blown films formulations.

	Extrusion-blown film	
	Twin-screw (pelletizing step) ⇨	Single-screw (film step)
	$T(^\circ C) = 120 - 130; N = 100$ rpm	$T(^\circ C) = 150 - 140; N = 60$ rpm
PBS	-	PBS
PBSax89		PBS + ax89
PBSnano	(PBS + D43B) = PBSnano	PBSnano
PBSax89nano	(PBS + D43B + ax89) = PBSax89nano	PBSax89nano
	$T(^\circ C) = 180 - 170; N = 82$ rpm	$T(^\circ C) = 180 - 165; N = 60$ rpm
PBSPLA	-	PBS + PLA
PBSPLAax89		PBS + ax89 + PLA
PBS-PLAnano	(PLA + D43B) = PLAnano	PBS+(PLAnano)
PBSax89-PLAnano		PBS + ax89 + (PLAnano)
PBSPLAax89nano	(PBS + ax89 + PLA + D43B) = PBSPLAax89nano	PBSPLAax89nano

15480585, 0, Downloaded from https://4spepublications.onlinelibrary.wiley.com/doi/10.1002/vnl.22092 by Ecole Polytech De Montreal, Wiley Online Library on [09/04/2024]. See the Terms and Conditions (https://onlinelibrary.wiley.com/terms-and-conditions) on Wiley Online Library for rules of use; OA articles are governed by the applicable Creative Commons License

2.3.3 | X-ray diffraction (XRD)

X-ray diffraction patterns for D43B and D43B-PLA/Plasticizers systems were obtained using an X-ray diffractometer (type Bruker D8 Advance, USA) with a copper source (Cu), operated at 40 kV and 40 mA. The measurements were carried out in the range 1–40° of 2θ, and the distance between the clay mineral layer was calculated from the Bragg law:

$$d = \frac{\lambda}{2\sin(\theta)} \quad (1)$$

where d represents the basal distance, θ the beam incidence angle and Λ the wavelength of x-ray used (1.54 Å).

2.3.4 | Differential scanning calorimetry (DSC)

The thermal parameters of PBS, PBSax89, PBS-PLA, PBSPLAax89 and its nanocomposites were determined using differential scanning calorimetry (DSC). The measurements were carried out in a Q2000 (TA instruments, USA) under a nitrogen atmosphere. First, the samples were heated from 0 to 200°C at a heating rate 10°C/min, followed by cooling to −80°C at a heating rate 20°C/min, and then by a second heating to 200°C at 10°C/min. Finally, a second cooling to bring the temperature within the apparatus to room temperature was performed.

2.3.5 | Oxygen permeability

Oxygen transmission was measured using a MOCON Ox-Tran 2/20 (Minneapolis, USA) with an oxygen flow rate of 20 sccm, at 0% relative humidity, room temperature, and under atmospheric conditions. Minimum two tests were performed for each sample with a surface of 100 cm^2 and a thickness around 55 µm.

2.3.6 | Tensile mechanical testing

Tensile mechanical tests were performed to determine the mechanical behavior of the nanocomposites blown films. Testing was carried on an instron (Norwood, MA) 3365 universal testing machine with a 500 N load cell. The tensile modulus and elongation at break were measured at room temperature. The measurements were performed based on ASTM D882.

3 | RESULTS AND DISCUSSION

3.1 | Structure and morphology

To investigate the phase morphology of PBSax89, PBSPLA, and PBSPLAax89 blends, and its nanocomposites, SEM observations were performed on the cryo-fractured surfaces of the different samples, after coating with a 15 nm thick gold layer.

In Figure 1A, a co-continuous morphology is observed that could indicate a potential reaction between PBS and ax89.[10] The PBSPLAax89 blend showed a similar result (Figure 1D), indicating an increase in compatibility between PBS and PLA after adding ax89. In fact, the small nodules and cavities observed in the PBSPLA blend[18] (Figure 1C) showing a non miscible mixture were eliminated by the presence of the reactive compatibilizer ax89.

In the case of PBSax89nano, PBSPLAax89nano, and PBSax89-PLAnano nanocomposites, nodular structures were observed as shown in Figure 1B,E,F. It is possible that D43B prevented the reactive effect of ax89 with the two matrices, resulting in a reduction in compatibility between PBS and PLA. A similar morphology was also obtained by PBS-PLAnano nanocomposite, confirming no effect of D43B on the compatibility of PBS with PLA.

A comparison of TEM images (Figure 2) between PBSPLAax89nano and PBSax89-PLAnano nanocomposites was performed to determine if the blending sequence has any impact on the polymers phase morphology. In the PBSPLAax89nano system, the D43B has been located at the PBS-PLA interface, which is the ax89 phase. This is an indication that ax89 is highly compatible with D43B, which prevents its reaction with polymers. Whereas, for PBSax89-PLAnano, the prior mixing of D43B with PLA was induced to preserve the organomontmorillonite D43B in the PLA phase.[3,4]

3.2 | Dispersion state of D43B in PBS and PBSPLA nanocomposites films

The dispersion state of D43B was evaluated in different matrices using XRD measurements and TEM observations. Figure 3 shows XRD patterns of D43B and different nanocomposite films, in the range of 1–10°. The characteristic diffraction peak of D43B is located at 4.8°, which corresponds to a basal distance (d_{001}) of 1.84 nm. Similar results were reported in the literature.[19] A significant shift in its characteristic peak at a low angle was recorded after its incorporated into PBS matrix, which suggests the formation of an intercalated structure. Adding 5 wt% of reactive compatibilizer ax89 resulted in an increase in

15480585, 0, Downloaded from https://4spepublications.onlinelibrary.wiley.com/doi/10.1002/vnl.22092 by Ecole Polytech De Montreal, Wiley Online Library on [09/04/2024]. See the Terms and Conditions (https://onlinelibrary.wiley.com/terms-and-conditions) on Wiley Online Library for rules of use; OA articles are governed by the applicable Creative Commons License

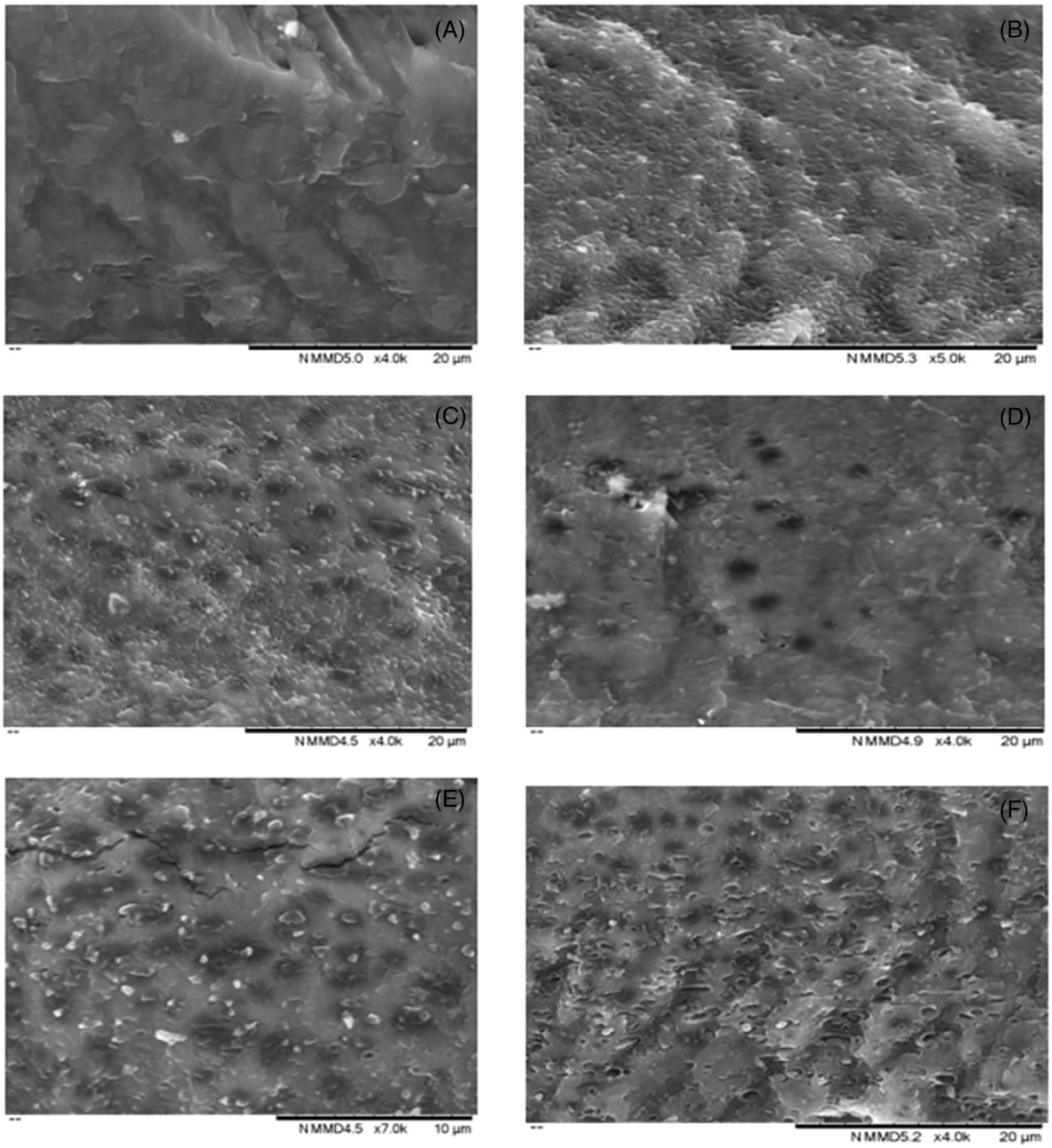

FIGURE 1 SEM images of: (A) PBSax89; (B) PBSax89nano; (C) PBSPLA; (D) PBSPLAax89; (E) PBS-PLAnano; and (F) PBSPLAax89nano (PBSax89-PLAnano).

this displacement. In fact, the reflection peak of D43B moved to 2.91° and 2.53°, which corresponds to basal distances of 3.03 and 3.49 nm for PBSnano and PBSax89-nano nanocomposites films, respectively. Concerning PBS-PLAnano and PBSax89-PLAnano (PBSPLAax89nano) nanocomposites films, displacements of 2.58° and 2.61°, respectively, corresponding to the basal distances of 3.42 and 3.38 nm, respectively; were observed. These results corroborate those found by SEM images, thus supporting the hypothesis that D43B presents a higher compatibility with ax89 than with PLA or PBS.

The TEM micrographs presented in Figure 4 confirm the results reported by SEM analysis and XRD diffraction. Indeed, intercalation layers of D43B can be clearly observed in the various nanocomposites. Concerning its location, the layers of D43B are mainly located in the PLA phase for PBS-PLAnano, as shown in Figure 4C. PBSax89-PLAnano nanocomposite film showed a similar observation with some layers near the interface of PLA-ax89 (Figure 4D). Whereas, for PBSPLAax89nano nanocomposite, fine dark lines appeared at the interface region of PBS-PLA (ax89 phase) (Figure 4E).

15480585, 0, Downloaded from https://4spepublications.onlinelibrary.wiley.com/doi/10.1002/vnl.22092 by Ecole Polytech De Montreal, Wiley Online Library on [09/04/2024]. See the Terms and Conditions (https://onlinelibrary.wiley.com/terms-and-conditions) on Wiley Online Library for rules of use; OA articles are governed by the applicable Creative Commons License

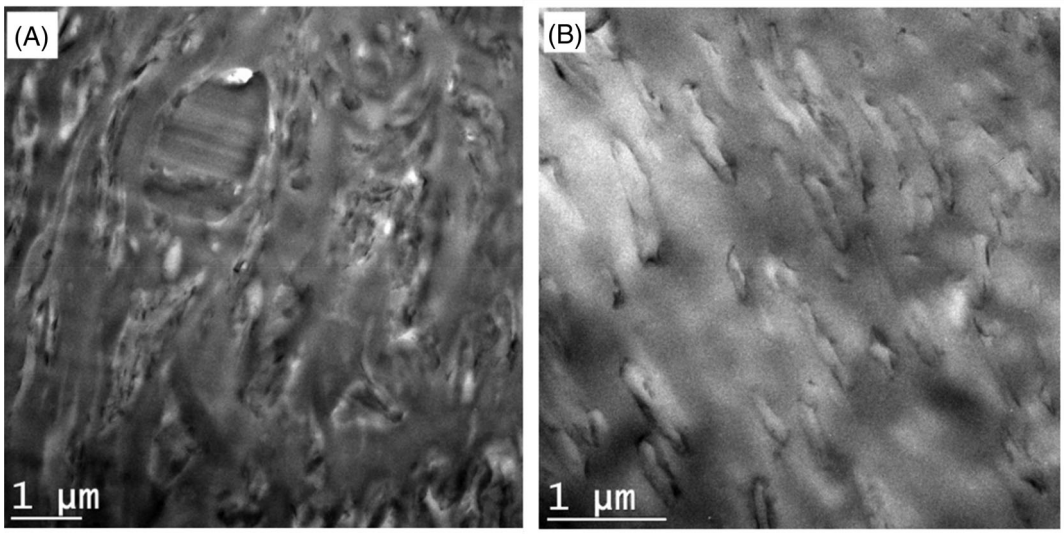

FIGURE 2 TEM images of: (A) PBSax89-PLAnano and (B) PBSPLAax89nano.

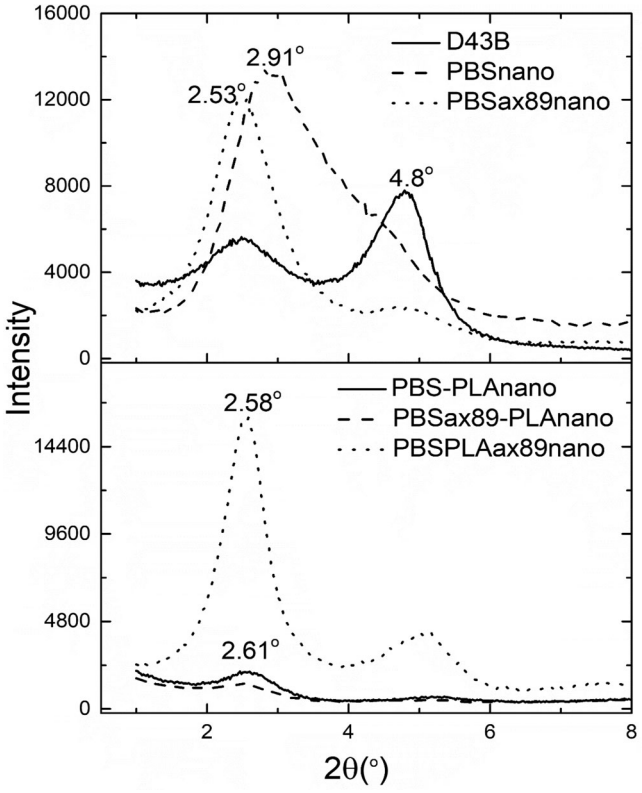

FIGURE 3 XRD diffraction: D43B and PBS (PBS/PLA) nanocomposites blown films at 0–10°.

3.3 | Thermal parameters

The thermal parameters of PBS, PBSax89, PBS blends and its nanocomposites from second heating are reported in the Figures 5, 6, and Table 3. As shown in Figure 5, PBS presents a transition temperature (T_g) and a melting temperature (T_m) at −45 and 87°C, respectively. The value of $T_{m(PBS)}$ suggests that it is rather the copoly(butylene succinate-co-butylene adipate) (PBSA),[18] with a fraction around 25% on butylene adipate (PBA). In fact, usually PBS has a melting temperature higher than 100,[3,6] but it can be reduced by adding a fraction of PBA.[6,7,10] No change in these temperatures was recorded after adding the D43B and/or the ax89 to PBS. This result can be related to the poor compatibility between D43B and PBS. It is reduced more after addition of ax89 which presented high interactions with this organomontmorillonite.[20] The crystalline content $X_C(\%)$ was determined using Equation (2). Where: $\Delta H^0_m = 142\,J/g$ and W_{PBS} are enthalpy of PBSA 100% crystalline[21] and its weight percentage in the different blends and nanocomposites.

$$X_C(\%) = \frac{\Delta H_m}{(W_{PBS})\Delta H^0_m} \times 100 \quad (2)$$

The addition of D43B to the PBS matrix slightly reduced its crystalline content, especially in the presence of the reactive compatibilizer ax89, resulting in a 5% decrease. This can be related to the poor compatibility of PBS with D43B. Indeed, in our previous study, it was reported that the crystallinity of a polymer can be affected more by its compatibility with the organomontmorillonite than by the dispersion paramter.[20] In addition, the high compatibility between D43B and ax89, reduce more the contact PBS-D43B and prevent the reaction between epoxy groups of ax89 and hydroxyl groups of PBS.[10] The slight increase of crystalline content of PBS-PLAnano nanocomposite can be due to the high compatibility of D43B with PLA matrix.[20] Similar results were

15480585, 0, Downloaded from https://4spepublications.onlinelibrary.wiley.com/doi/10.1002/vnl.22092 by Ecole Polytech De Montreal, Wiley Online Library on [09/04/2024]. See the Terms and Conditions (https://onlinelibrary.wiley.com/terms-and-conditions) on Wiley Online Library for rules of use; OA articles are governed by the applicable Creative Commons License

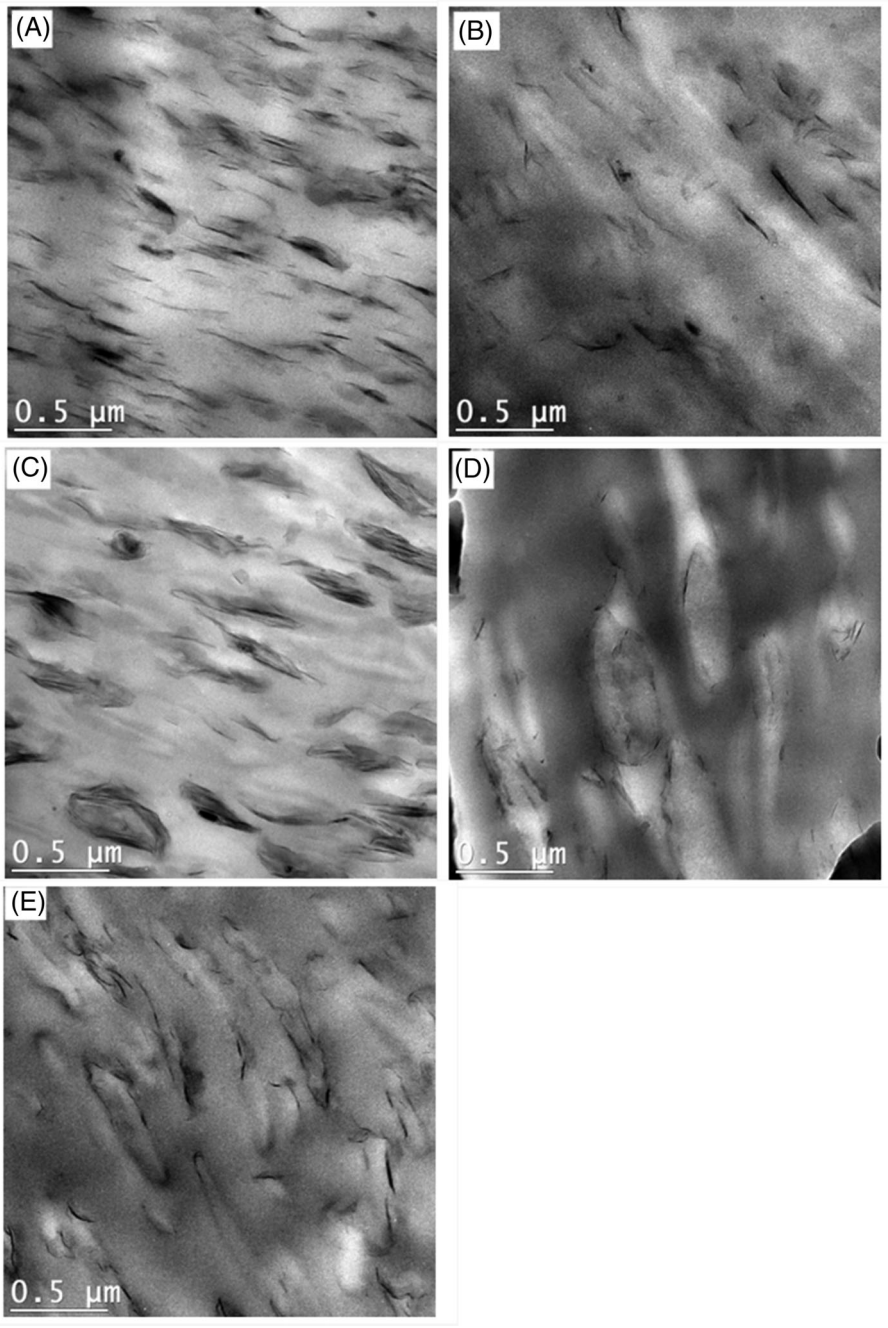

FIGURE 4 TEM images of: (A) PBSnano, (B) PBSax89nano, (C) PBS-PLAnano, (D) PBSax89-PLAnano, and (E) PBSPLAax89nano.

observed for PBSPLAax89nano and PBSax89-PLAnano nanocomposites (Table 3).

3.4 | Oxygen permeability

The neat and nanocomposites films of PBS, PBSax89, PBS-PLA, and PBSPLAax89 were characterized by oxygen permeability (P_{O_2}) tests, under a $T_{ambient}$, RH = 0% and $P_{atmosphere}$ conditions. PBS and PLA[20] presented respectively a permeability at 1008 cc.mil/m^2 day atm and 1102 cc.mil/m^2 day atm. A negligible increase of P_{O_2} was observed after adding 3 wt% of D43B into PBS matrix. A similar result was obtained by PBSax89nano nanocomposite. The reason for this is the low compatibility between D43B and PBS,[20] despite its good dispersion in the matrix, especially after adding 5 wt% of ax89. This result corroborates with the previous analysis (XRD diffraction, SEM, and TEM images and thermal parameters). A higher permeability was reported by PBSPLA blend. Indeed, an increase of 50% of P_{O_2} was induced at the addition of 30 wt% of PLA to PBS. This can be due to the immiscibility of PBS with PLA, which caused a decrease of crystallinity by increasing the free volume inside PBS

15480585, 0, Downloaded from https://4spepublications.onlinelibrary.wiley.com/doi/10.1002/vnl.22092 by Ecole Polytech De Montreal, Wiley Online Library on [09/04/2024]. See the Terms and Conditions (https://onlinelibrary.wiley.com/terms-and-conditions) on Wiley Online Library for rules of use; OA articles are governed by the applicable Creative Commons License

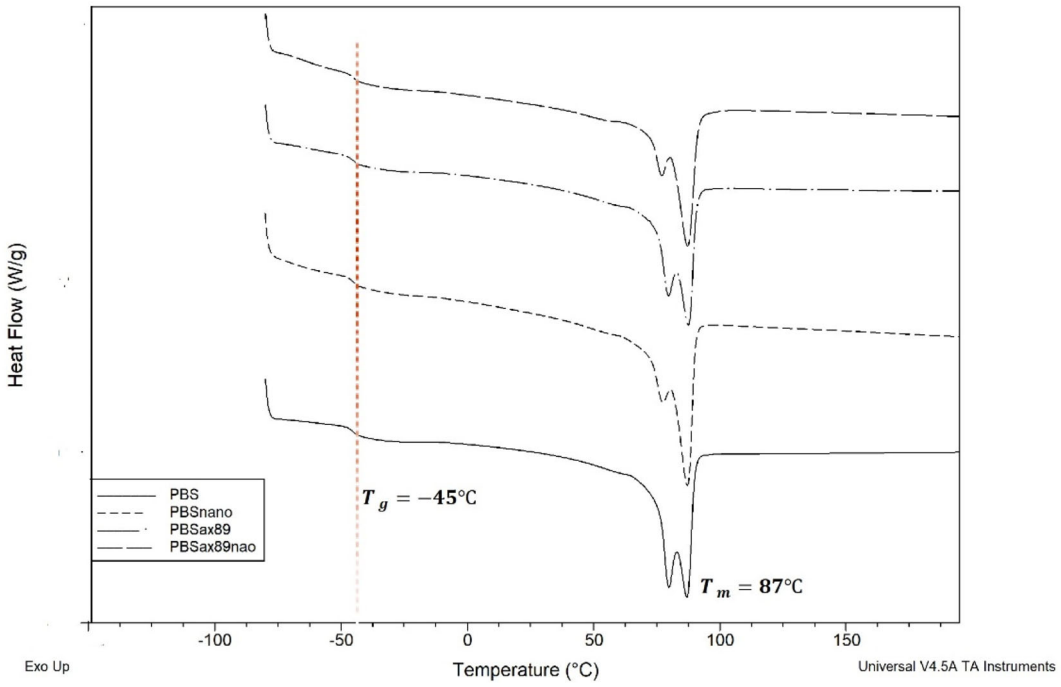

FIGURE 5 DSC heating thermograms of PBS, PBSax89 blend, PBSnano, and PBSax89nano nanocomposite films.

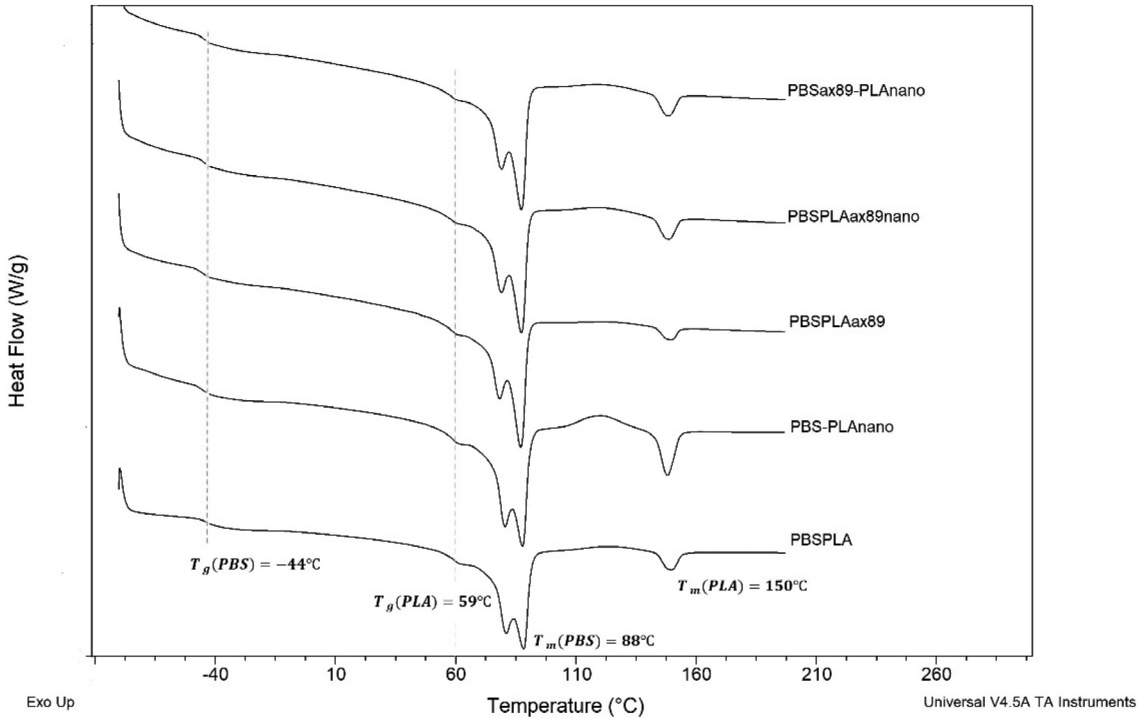

FIGURE 6 DSC heating thermograms of PBSPLA, PBSPLAax89 blend, PBS-PLAnano, PBSPLAax89nano, and PBSax89-PLAnano nanocomposite films.

matrix. Nevertheless, the introduction of 5 wt% of the reactive compatibilizer ax89 to the PBS-PLA blend resulted in an approximately 38% reduction in oxygen permeability. This reduction may be attributed to the potential reaction between the epoxy groups of ax89 and the hydroxyl groups present in PBS and PLA, thereby enhancing compatibility between PBS and PLA.[6] A greater reduction of oxygen permeability was obtained by

15480585, 0, Downloaded from https://4spepublications.onlinelibrary.wiley.com/doi/10.1002/vnl.22092 by Ecole Polytech De Montreal, Wiley Online Library on [09/04/2024]. See the Terms and Conditions (https://onlinelibrary.wiley.com/terms-and-conditions) on Wiley Online Library for rules of use; OA articles are governed by the applicable Creative Commons License

PBS-PLAnano nanocomposite. This result can be associated to two parameters. The first one is the high compatibility of D43B with PLA matrix, which can affect directly the crystallinity of this phase, as reported in the previous study.[20] The second parameter concerns the choice of mixing method.[22] In fact, the prior mixing of D43B with PLA was induced to preserve the organomontmorillonite D43B in the PLA phase and prevents the encapsulation effect by PBS phase to happen.[3,4] Moreover, the greatest increase in oxygen barrier was obtained after adding 5 wt% of ax89 to the PBS-PLAnano system, thus increasing the compatibility between PBS and PLA (Figure 7).

3.5 | Mechanical tests

The tensile modulus and the elongation at the break of neat PBS, PBS blends and its nanocomposites are presented in Figures 8 and 9. The tensile modulus and elongation at the break of PBS in machine direction (MD) were found as 195 ± 45 MPa and at 620 ± 55%, respectively, due to its ductile nature.[21] Unlike PBS, PLA is brittle, with a high tensile modulus and low elongation at break, measured at 1153 ± 71 MPa and 29.5 ± 5%, respectively, as reported in the previous study.[23]

Figure 8 shows an increase in the elongation at break in case of PBSax89 system, particularly in the transverse direction (TD). In contrast, addition of 3 wt% of D43B resulted in a decrease in PBS elongation at break, specifically in the machine direction (MD). This phenomenon can be explained by the strong compatibility exhibited between PBS and ax89, which suggests the potential occurrence of chemical reactions between the epoxy groups of ax89 and the hydroxyl groups within PBS,[5] as validated by prior analyses. On the other hand, the reduction in elongation can be attributed to the limited compatibility observed between this organo-montmorillonite and PBS. A significant reduction in elongation at break in the machine direction was observed in the PBSax89-nano system, with a reported value of 364 ± 25%, while no change was observed in the transverse direction (TD). This observation may be attributed to the inhibitory

TABLE 3 Thermal parameters of PBS, PBS blends, and its nanocomposites.

	Second heating				
	T_g(°C)	T_m(°C)	ΔH_m (J/g)	PBS (wt%)	X_c(%)
PBS	−45	87	38.83	100	27
PBSax89	−46	87	35.11	95	26
PBSnano	−45	88	33.16	97	24
PBSax89nano	−45	87	29.36	92	22
PBSPLA	−44	88	16.42	70	17
PBSPLAax89	−46	87	19.23	70	19
PBS-PLAnano	−45	88	20.18	70	20
PBSPLAax89nano	−43	87	19.63	70	20
PBSax89-PLAnano	−43	87	19.10	70	19

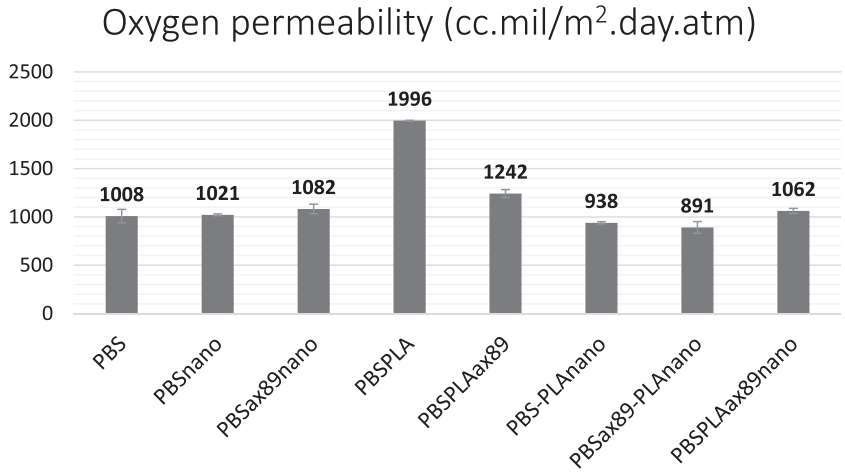

FIGURE 7 Oxygen permeability of neat and nanocomposite films of PBS, PBSax89, PBS-PLA, and PBSPLAax89.

15480585, 0, Downloaded from https://4spepublications.onlinelibrary.wiley.com/doi/10.1002/vnl.22092 by Ecole Polytech De Montreal, Wiley Online Library on [09/04/2024]. See the Terms and Conditions (https://onlinelibrary.wiley.com/terms-and-conditions) on Wiley Online Library for rules of use; OA articles are governed by the applicable Creative Commons License

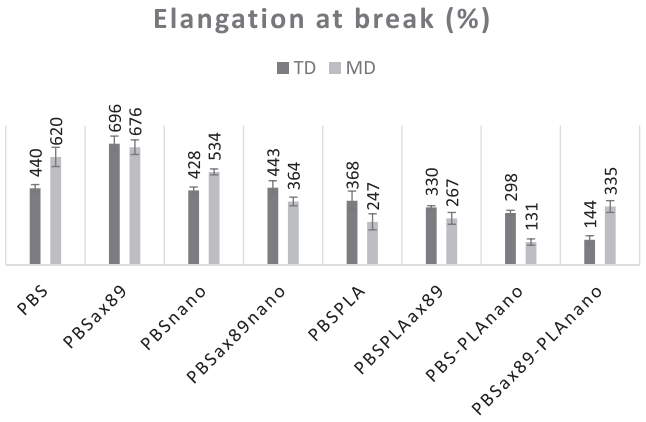

FIGURE 8 Elongations at break of: PBS, PBS blends, and PBS nanocomposites.

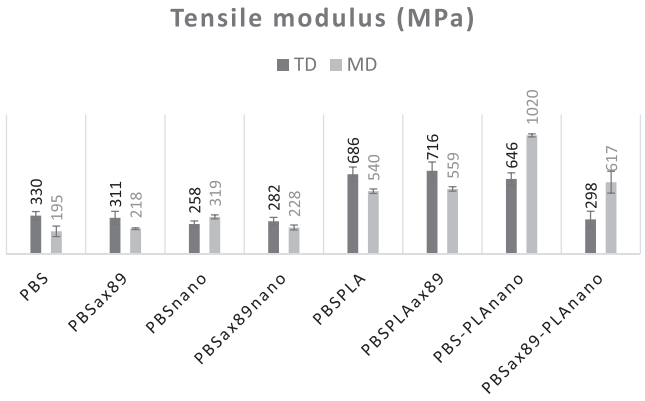

FIGURE 9 Tensile modulus of: PBS, PBS blends, and PBS nanocomposites.

effect of D43B, which seems to impede the interaction between the reactive compatibilizer ax89 and PBS.

In the case of the PBS-PLA blend, a notable reduction in elongation at break was observed in both machine (MD) and transverse (TD) directions. This decrease can be attributed to the limited compatibility between PBS and PLA, which leads to inadequate interfacial adhesion between these two polymer phases. The incorporation of 5 wt% of ax89 into the PBS-PLA blend resulted in a moderate increase in elongation at break in the MD direction. This increase can be attributed to the potential interaction between ax89 and PBS, effectively enhancing the flexibility of the PBS component.[5] However, it is essential to note that a small decrease in the TD direction was observed, possibly due to the limited reactivity of ax89 with PLA, which did not enhance its ductility in that particular direction. A more significant decrease in elongation was observed in the case of PBS-PLAnano. This decrease can be attributed to the poor compatibility of D43B with PBS, as well as its presence in the PLA phase, resulting in a notable increase in interfacial separation between PBS and PLA. However, the introduction of ax89 into the PBS-PLAnano system resulted in an increase in elongation in the machine direction (MD). This can be due to the possible reaction between PBS and ax89. In fact, the PBSax89-PLAnano nanocomposites exhibited a MD elongation of 335 ± 34%.

In Figure 9, an increase in PBS tensile modulus with the addition of ax89 or D43B in the machine direction was observed, coupled with a decrease in the transverse direction. For PBSnano, this increase in the machine direction is attributed to the alignment of organomontmorillonite (OMMt) nanoparticles, enhancing load-bearing capacity. Conversely, OMMt nanoparticles have less constraint on polymer chain mobility in the transverse direction, resulting in greater flexibility and lower tensile modulus. In the case of the PBSax89 system, the addition of a reactive plasticizer reduces tensile modulus in the transverse direction by increasing chain mobility and reducing intermolecular interactions. However, in the machine direction, the plasticizer enhances chain alignment, forms a crosslinking network, and achieves a more uniform molecular weight distribution, leading to an increased tensile modulus.

In the PBS-PLA blend, there is a significant increase in modulus in both directions. The addition of ax89 further enhances the modulus in both directions. However, in the PBS-PLAnano system, a substantial increase is observed in the machine direction, with minimal change in the transverse direction. For PBSax89-PLAnano, there is a marked decrease in modulus in the transverse direction, but in the machine direction, it remains higher than for the PBS-PLA and PBS-PLAax89 systems. This suggests that interactions between additives and blend components are crucial in determining material properties, underlining the delicate balance required to achieve desired characteristics for specific applications.[3,6]

4 | CONCLUSION

In conclusion, the investigation utilizing SEM, TEM, and XRD techniques shed light on the interplay between D43B and ax89 and their effects on the properties of PBS and PLA blends. SEM analysis pointed to enhanced compatibility between PBS and PLA in the presence of ax89, resulting in the formation of a co-continuous structure. However, the emergence of nodular structures in the nanocomposites suggested compromised compatibility, attributed to the influence of D43B.

Oxygen permeability tests revealed no changes in PBS with the addition of D43B, with and without the presence of ax89. The PBS/PLA blend exhibited a notable 50%

15480585, 0, Downloaded from https://4spepublications.onlinelibrary.wiley.com/doi/10.1002/vnl.22092 by Ecole Polytech De Montreal, Wiley Online Library on [09/04/2024]. See the Terms and Conditions (https://onlinelibrary.wiley.com/terms-and-conditions) on Wiley Online Library for rules of use; OA articles are governed by the applicable Creative Commons License

increase in permeability compared to PBS, attributed to immiscibility. However, the introduction of ax89 played a crucial role in enhancing compatibility, resulting in a significant 38% reduction in oxygen permeability with a 5 wt% addition. The PBS-PLAnano nanocomposite demonstrated an even greater reduction of approximately 47%, due to high compatibility between D43B and PLA, further improved by a selective mixing method. The addition of ax89 to PBS-PLAnano led to an enhanced reduction of around 53%.

Concerning the mechanical properties, the addition of ax89 increased the elongation at break of PBS, especially in the transverse direction. However, the presence of D43B, particularly after adding 5 wt% ax89, resulted in a 41% decrease in elongation in the MD. In the PBS-PLAnano system, compared to the PBS-PLA film, a reduction in elongation at the break was also observed, especially in the MD, dropping from 247 ± 46 to 131 ± 18 in the presence of D43B. This result is due to the poor compatibility of D43B with PBS and its presence in the PLA phase, where a synergistic effect was produced between D43B and PLA, resulting in high compatibility between the two. Nevertheless, the inclusion of 5 wt% ax89 contributed to the increase of elongation (MD) of the nanocomposite by around 60%.

Overall, these findings underscore the intricate balance required between additives and blend components to achieve the desired material properties, emphasizing the complexity involved in tailoring specific characteristics for diverse application requirements.

ACKNOWLEDGMENTS

The authors would like to thank the CREPEC researches associates (M.Sc.A): Claire Cercle, Richard Silverwood, and Matthieu Gauthier for their help on all analysis realized in this work. The authors would like also to acknowledge financial support of NSERC and Polyexpert Inc. through the CRD program.

CONFLICT OF INTEREST STATEMENT

The authors declare no competing interests.

DATA AVAILABILITY STATEMENT

Data sharing is not applicable to this article as no new data were created or analyzed in this study.

ORCID

Salima Adrar https://orcid.org/0000-0002-0251-9127

REFERENCES

1. Zeng J-B, Li K-A, Du A-K. Compatibilization strategies in poly(lactic acid)-based blends. *RSC Adv*. 2015;5(41):32546-32565. doi:10.1039/C5RA01655J
2. Su S, Kopitzky R, Tolga S, Kabasci S. Polylactide (PLA) and its blends with poly(butylene succinate) (PBS): a brief review. *Polymers*. 2019;11(7):7. doi:10.3390/polym11071193
3. Barletta M, Aversa C, Ayyoob M, et al. Poly(butylene succinate) (PBS): materials, processing, and industrial applications. *Prog Polym Sci*. 2022;132:101579.
4. Xu J, Manepalli PH, Zhu L, Narayan-Sarathy S, Alavi S. Morphological, barrier and mechanical properties of films from poly(butylene succinate) reinforced with nanocrystalline cellulose and chitin whiskers using melt extrusion. *J Polym Res*. 2019;26:1-10.
5. Zhao X, Zhang D, Yu S, Zhou H, Peng S. Recent advances in compatibility and toughness of poly(lactic acid)/poly(butylene succinate) blends. *E-Polym*. 2021;21(1):793-810. doi:10.1515/epoly-2021-0072
6. Palai B, Mohanty S, Nayak SK. Synergistic effect of polylactic acid (PLA) and poly(butylene succinate-co-adipate) (PBSA) based sustainable, reactive, super toughened eco-composite blown films for flexible packaging applications. *Polym Test*. 2020;83:106130.
7. Harada M, Ohya T, Iida K, Hayashi H, Hirano K, Fukuda H. Increased impact strength of biodegradable poly(lactic acid)/poly(butylene succinate) blend composites by using isocyanate as a reactive processing agent. *J Appl Polym Sci*. 2007;106(3):1813-1820. doi:10.1002/app.26717
8. Hu X, Su T, Li P, Wang Z. Blending modification of PBS/PLA and its enzymatic degradation. *Polym Bull*. 2018;75:533-546.
9. Jiang G, Wang H, Yu L, Li H. Improving crystallization properties of PBSA by blending PBS as a polymeric nucleating agent to prepare high-performance PPC/PBSA/AX8900 blown films. *Polym Eng Sci*. 2022;62(4):1166-1177. doi:10.1002/pen.25915
10. Xue B, He H, Zhu Z, et al. A facile fabrication of high toughness poly(lactic acid) via reactive extrusion with poly(butylene succinate) and ethylene-methyl acrylate-glycidyl methacrylate. *Polymers*. 2018;10(12):1401.
11. T. Messin, S. Marais, N. Follain, A. Guinault, V. Gaucher, N. Delpouve, C. Sollogoub, "Biodegradable PLA/PBS multinanolayer membrane with enhanced barrier performances," *J Membr Sci*, vol. 598, p. 117777, 2020, doi: 10.1016/j.memsci.2019.117777
12. Zhou S-Y, Huang HD, Ji X, et al. Super-robust polylactide barrier films by building densely oriented lamellae incorporated with ductile in situ nanofibrils of poly(butylene adipate-co-terephthalate). *ACS Appl Mater Interfaces*. 2016;8(12):8096-8109. doi:10.1021/acsami.6b00451
13. Zhou S-Y, Huang HD, Xu L, et al. In situ nanofibrillar networks composed of densely oriented polylactide crystals as efficient reinforcement and promising barrier wall for fully biodegradable poly(butylene succinate) composite films. *ACS Sustain Chem Eng*. 2016;4(5):2887-2897. doi:10.1021/acssuschemeng.6b00590
14. Xie L, Xu H, Chen JB, et al. From nanofibrillar to nanolaminar poly(butylene succinate): paving the way to robust barrier and mechanical properties for full-biodegradable poly(lactic acid) films. *ACS Appl Mater Interfaces*. 2015;7(15):8023-8032. doi:10.1021/acsami.5b00294
15. Kakroodi AR, Kazemi Y, Nofar M, Park CB. Tailoring poly(lactic acid) for packaging applications via the production

15480585, 0, Downloaded from https://4spepublications.onlinelibrary.wiley.com/doi/10.1002/vnl.22092 by Ecole Polytech De Montreal, Wiley Online Library on [09/04/2024]. See the Terms and Conditions (https://onlinelibrary.wiley.com/terms-and-conditions) on Wiley Online Library for rules of use; OA articles are governed by the applicable Creative Commons License

of fully bio-based in situ microfibrillar composite films. *Chem Eng J*. 2017;308:772-782. doi:10.1016/j.cej.2016.09.130

16. Kakroodi AR, Kazemi Y, Rodrigue D, Park CB. Facile production of biodegradable PCL/PLA in situ nanofibrillar composites with unprecedented compatibility between the blend components. *Chem Eng J*. 2018;351:976-984. doi:10.1016/j.cej.2018.06.152
17. Messin T, Follain N, Guinault A, et al. Structure and barrier properties of multinanolayered biodegradable PLA/PBSA films: confinement effect via forced assembly coextrusion. *ACS Appl Mater Interfaces*. 2017;9(34):29101-29112. doi:10.1021/acsami.7b08404
18. Puekpoonpoal N, Phattarateera S, Kerddonfag N, Aht-Ong D. Morphology development of PLAs with different stereoregularities in ternary blend PBSA/PBS/PLA films. *Polym Plast Technol Mater*. 2021;60:1-14. doi:10.1080/25740881.2021.1930043
19. Araújo A, Botelho G, Oliveira M, Machado AV. Influence of clay organic modifier on the thermal-stability of PLA based nanocomposites. *Appl Clay Sci*. 2014;88:144-150.
20. Adrar S, Ajji A. Effect of different type of organomontmorillonites on oxygen permeability of PLA-based nanocomposites blown films. *Polym Eng Sci*. 2022;62(11):3796-3808. doi:10.1002/pen.26145
21. Seggiani M, Altieri R, Cinelli P, Esposito A, Lazzeri A. Thermoplastic blends based on poly(butylene succinate-co-adipate) and different collagen hydrolysates from tanning industry: I—Processing and thermo-mechanical properties. *J Polym Environ*. 2021;29(2):392-403. doi:10.1007/s10924-020-01880-y
22. Garofalo E, Di Maio L, Scarfato P, Russo P, Incarnato L. Selective localization of nanoparticles to enhance the properties of PBS/PLA nanocomposite blown films. *J Polym Environ*. 2023;31(10):4546-4558. doi:10.1007/s10924-023-02883-1
23. Adrar S, Ajji A. Interactions between PLA, organomontmorillonite and plasticizer: synergistic effect on the barrier and mechanical properties of PLA nanocomposites blown films. *J Appl Polym Sci*. 2024;141(4):e54867. doi:10.1002/app.54867

How to cite this article: Adrar S, Ajji A. Effect of blending sequence and epoxy functionalized compatibilizer on barrier and mechanical properties of PBS and PBS/PLA nanocomposite blown films. *J Vinyl Addit Technol*. 2024;1-12. doi:10.1002/vnl.22092

15480585, 0, Downloaded from https://4spepublications.onlinelibrary.wiley.com/doi/10.1002/vnl.22092 by Ecole Polytech De Montreal, Wiley Online Library on [09/04/2024]. See the Terms and Conditions (https://onlinelibrary.wiley.com/terms-and-conditions) on Wiley Online Library for rules of use; OA articles are governed by the applicable Creative Commons License